

TWENTYFIFTH EUROPEAN ROTORCRAFT FORUM

Paper n° H5

**INFLOW MODEL FOR SIMULATION OF HELICOPTER FLIGHT
IN DYNAMIC GROUND EFFECT**

BY

H. XIN

J.V.R. PRASAD

D. A. PETERS

GEORGIA INSTITUTE OF TECHNOLOGY

WASHINGTON UNIVERSITY

USA

SEPTEMBER 14-16, 1999

R O M E

I T A L Y

ASSOCIAZIONE INDUSTRIE PER L' AEROSPAZIO, I SISTEMI E LA DIFESA
ASSOCIAZIONE ITALIANA DI AERONAUTICA ED ASTRONAUTICA

INFLOW MODEL FOR SIMULATION OF HELICOPTER FLIGHT IN DYNAMIC GROUND EFFECT

H. Xin
Graduate Research Assistant
School of Aerospace Engineering
Georgia Institute of Technology
Atlanta, GA 30332-0150, USA.

J.V.R. Prasad
Professor

D. A. Peters
Professor
Department of Mechanical Engineering
Washington University
St. Louis, MO 63130-4899, USA

Abstract

A newly developed finite-state ground effect model has been extended to modeling of lifting rotors operating above a moving ground plane. In this dynamic ground effect model, the influence of the ground motion is represented by pressure perturbation in the flow field with a discontinuity across the ground plane. The interference velocity distribution at the rotor disk is related to the ground velocity distribution by a ground motion influence coefficient matrix, $[C]$. The rotor inflow distribution, average inflow and induced torque are computed and discussed for dynamic ground effect cases. Results indicate that the ground velocity affects the induced inflow at the rotor disk, and the influence of the ground velocity is not negligible for lightly loaded helicopter rotors at low hovering height. The results and discussion show that the present finite-state model for dynamic ground effect is qualitatively correct and quantitatively reasonable.

Nomenclature

$[A'_{jk}]$	influence coefficient matrix for ground interference velocity due to ground pressure
$[B'_{kn}]$	influence coefficient matrix for ground pressure due to rotor pressure
$[C'_{ji}]$	influence coefficient matrix for ground interference velocity due to ground velocity
C_T	rotor thrust coefficient
F	transformation function from rotor to ground ellipsoidal coordinate system
$[G'_{jn}]$	influence coefficient matrix for ground interference velocity due to rotor pressure
g	ground velocity, positive upward, dimensionless on ΩR
h	rotor height above ground plane, dimensionless on R
$[L'_{jn}]$	influence coefficient matrix of induced velocity due to rotor pressure
$[M]$	apparent mass matrix
\overline{P}	normalized associated Legendre function of first kind
\overline{Q}	normalized associated Legendre function of second kind
V_m	mass flow parameter, dimensionless on ΩR
w	normal component of rotor induced velocity at rotor disk, positive downward, dimensionless on ΩR
w_G	normal component of ground interference velocity at rotor disk, positive upward, dimensionless on ΩR
$\{\alpha'_j\}$	rotor induced velocity coefficients
$\{\beta'_j\}$	ground interference velocity coefficients
Φ_R	pressure perturbation due to rotor, dimensionless on $\rho\Omega^2 R^2$
Φ_G^D	pressure perturbation due to ground velocity, dimensionless on $\rho\Omega^2 R^2$
Φ_G^S	pressure perturbation due to ground, dimensionless on $\rho\Omega^2 R^2$
$\{\gamma'_j\}$	ground velocity coefficients
(v, η, ψ)	rotor ellipsoidal coordinates, dimensionless
$(\hat{v}, \hat{\eta}, \hat{\psi})$	ground ellipsoidal coordinates, dimensionless
$\{\sigma'_k\}$	ground pressure coefficients
$\{\tau'_n\}$	rotor pressure coefficients
Ω	rotor rotational speed
ω	oscillation frequency of ground heaving motion
ξ	non-dimensional coordinate along free-stream line, positive upstream

1. Introduction

Modern helicopters are often required to operate close to the ground and the aerodynamic behavior of a lifting rotor is greatly affected when flying in ground effect. In many operations, a naval helicopter has to maintain a steady hover closely above a moving ship deck, as shown in Figure 1. The motion of the ship deck may involve heaving, pitching and rolling. In such a case, the helicopter rotor is subject to dynamic ground effect. In dynamic ground effect, not only the static presence of the ground plane but also the motion of the ground plane may have influence on the inflow magnitude and distribution at the rotor disk. A systematic modeling of dynamic ground effect is presented in this paper.

Many investigations on rotor ground effect, both experimental and theoretical, have been carried out in the past. As shown in Figure 2, Newman^[1] and Hayden^[2] correlated test data to obtain empirical relations of the in-ground-effect average inflow for hovering, where h is the hovering height normalized with respect to rotor radius. Almost all of the previous theoretical studies used various forms of the image rotor method, which guarantee that the boundary condition is automatically satisfied at the ground plane. As shown in Figure 2, Cheeseman's image rotor method^[3] gives good prediction except at very low hovering heights.

The 'Peters-He' generalized dynamic wake theory^[4] represents the induced inflow distribution at the rotor disk as a system of first order differential equations in time domain. Due to its dynamic nature and computational efficiency, the generalized dynamic wake theory is finding a wide application in flight dynamics and aeroelasticity analyses of rotorcraft. It has been implemented in major flight simulation programs currently used in helicopter industry. However, those models use empirical factors to account for ground effect and they cannot accurately predict in-ground effect inflow distributions for cases such as dynamic ground effect, etc. Thus, there is a definite need for development of a finite-state ground effect model for general ground effect cases.

A new finite-state ground effect model^[5] has recently been developed for lifting rotors based on the generalized dynamic wake theory. The influence of the ground plane is represented as a second spatially distributed pressure perturbation in the flow field. The total perturbation potential, which determines the induced inflow at rotor disk, is obtained as the superposition of both the rotor and the ground contributions. In Figure 3, the normalized average inflow at the rotor disk predicted using the new finite-state ground effect model, taken from Ref. [5], is shown. The results obtained using Newman's and Hayden's empirical methods are also shown in the same figure. It can be seen from Figure 3 that the current model is able to predict as well as the Cheeseman's image rotor model for the normal ground effect case. Especially for low values of rotor height above the ground plane ($h < 0.4$), the current model predictions are better than those of the Cheeseman's image rotor model. This model has been extended to the modeling of a helicopter hovering above an inclined ground plane in reference [6]. In this paper, the new finite-state ground effect model is extended for modeling of dynamic ground effect.

2. Background and Basic Equations

The generalized dynamic wake theory^[4] was developed for an incompressible potential flow with small perturbations relative to the free stream. In such a case, the pressure perturbation due to a lifting rotor, Φ_R , can be treated as the acceleration potential that satisfies Laplace's equation and the zero-pressure perturbation condition at infinity. When written in an ellipsoidal coordinate system with origin at the rotor disk center, a suitable general solution for the acceleration potential can be obtained using the method of separation of variables as

$$\Phi_R = -\frac{1}{2} \sum_{m=0}^{\infty} \sum_{n=m+1, m+3, \dots}^{\infty} \bar{P}_n^m(v) \bar{Q}_n^m(i\eta) [\tau_n^{m,c} \cos(m\psi) + \tau_n^{m,s} \sin(m\psi)] \quad (1)$$

where $\bar{P}_n^m(i\eta)$ and $\bar{Q}_n^m(i\eta)$ are normalized associated Legendre functions of the first and second kind, respectively. Since v is positive above the disk and negative below the disk, the above pressure function Φ_R with $n+m$ odd yields a discontinuity in pressure across the rotor disk where $\eta = 0$. Therefore, the rotor disk loading can be obtained as the pressure difference between the upper and the lower surfaces of the disk.

If the induced velocity distribution at the rotor disk is expanded in terms of a set of azimuthal harmonics and radial shape functions with unknown coefficients,

$$w = \sum_r \sum_j P_j^r(v) [\alpha_j^{r,c}(t) \cos(r\psi) + \alpha_j^{r,s}(t) \sin(r\psi)] \quad (2)$$

the rotor pressure coefficients $\{\tau\}$ and the inflow coefficients $\{\alpha\}$ can be related using a matrix representation as

$$[M] \{\alpha\} + V_m [L]^{-1} \{\alpha\} = \left\{ \frac{\tau}{2} \right\} \quad (3)$$

where, the $[M]$ matrix is called the apparent mass matrix, V_m is the mass flow parameter, and the $[L]$ matrix is the induced inflow influence coefficient matrix. With the $[L]$ matrix and mass flow parameter, one can obtain the quasi-steady part of the induced inflow at the rotor disk for a given load distribution,

$$\{a\} = \frac{1}{V_m} [L] \left\{ \frac{\tau}{2} \right\} \quad (4)$$

In reference [4], closed form expressions for the elements of the $[L]$ matrix were developed for out of ground effect flight conditions, and comparisons were made between theoretical predictions and measured inflow data.

In our approach to modeling of ground effect, a second pressure perturbation, Φ_G , is assumed to exist in the flow field due to the presence of the ground plane. For satisfying the Laplace's equation and the boundary condition at infinity, the pressure perturbation due to the ground is represented as

$$\Phi_G = \frac{1}{2} \sum_{l=0}^{\infty} \sum_{k \geq l} \bar{P}_k^l(\hat{v}) \bar{Q}_k^l(i\hat{\eta}) [\sigma_k^{lc} \cos(l\hat{\psi}) + \sigma_k^{ls} \sin(l\hat{\psi})] \quad (5)$$

where, the associated Legendre functions are now expressed in another ellipsoidal coordinate system $(\hat{v}, \hat{\eta}, \hat{\psi})$ with its origin at the center of the rotor wake footprint on the ground plane. The transformation between the rotor and the ground ellipsoidal coordinate systems, i.e.,

$$(\hat{v}, \hat{\eta}, \hat{\psi}) = F(v, \eta, \psi) \quad (6a)$$

and its inverse

$$(v, \eta, \psi) = F^{-1}(\hat{v}, \hat{\eta}, \hat{\psi}) \quad (6b)$$

are determined by flight condition as well as relevant parameters such as the normalized rotor height above the ground plane, h , the tip-path-plane angle of attack, α_{TPP} , the helicopter heading angle, Ψ , the ground plane inclination angle, δ , and the effective wake skew angle, χ_e , as defined in references [5] and [6].

In equation (5), the pressure perturbation can be represented as either a source-like distribution ($k + l$ even) or a pressure-jump ($k + l$ odd) at the ground, each simulating the momentum change due to turning the flow by the ground plane. However, the source-like distribution is more reasonable since the flow is turned without energy loss, and hence, $k = l, l+2, l+4, \dots$ is used in the current study. With this expression, the ground pressure is continuous across the ground plane. By applying a pressure boundary condition at the ground plane, i.e.,

$$\Phi_G \Big|_{\hat{\eta}=0} = \Phi_R \Big|_{\hat{\eta}=0} \quad (7)$$

as well as the orthogonal properties of Legendre functions $\bar{P}_k^l(\hat{v})$'s, the ground pressure coefficients in equation (5) can be related to the rotor pressure coefficients in equation (1) as

$$\{\sigma_k^l\} = [B_{kn}^{lm}] \{\tau_n^m\} \quad \begin{array}{l} l, m = 0, 1, 2, \dots \\ k = l, l+2, l+4, \dots; n = m+1, m+3, \dots \end{array} \quad (8)$$

The elements of the $[B]$ matrix are determined by integration over the rotor wake footprint on ground plane with use of the coordinate transformation

$$(v, \eta, \psi) = F^{-1}(\hat{v}, \hat{\eta} = 0, \hat{\psi}) \quad (9)$$

In the new ground effect model, the ground effect on the induced inflow at the rotor disk is treated as an upward interference velocity, w_G . Thus, the in-ground-effect inflow velocity becomes

$$w^{IGE} = w - w_G \quad (10)$$

where w is the out-of-ground-effect induced velocity expressed as in equation (2) and is determined from equation (3) or (4). Analogous to the rotor induced velocity, the ground interference velocity can be expressed as

$$w_G = \sum_r \sum_{j=r+1, r+3, \dots} \bar{P}_j^r(v) [\beta_j^{rc} \cos(r\psi) + \beta_j^{rs} \sin(r\psi)] \quad (11)$$

The ground interference velocity coefficients can thus be related with the ground pressure coefficients by

$$\{\beta_j^r\} = \frac{1}{V_m} [A_{jk}^r] \left\{ \frac{\sigma_k^l}{2} \right\} \quad \begin{array}{l} l, r = 0, 1, 2, \dots \\ k = l, l+2, l+4, \dots; j = r+1, r+3, \dots \end{array} \quad (12)$$

The mass flow parameter in the above equation is assumed to be same as that for the out-of-ground-effect case in equations (3) and (4), since the ground does not alter the mass flow but only redirects the flow. Applying the orthogonal property of $\bar{P}_j^r(v)$'s at the rotor disk, i.e., $\eta = 0$, the elements of $[A]$ matrix are determined by integration over the rotor disk with use of the transformation

$$(\hat{v}, \hat{\eta}, \hat{\psi}) = F(v, \eta = 0, \psi) \quad (13)$$

Combining equations (9) and (12), we have the relationship between the ground interference velocity coefficients and the rotor pressure coefficients in a matrix form as

$$\{\beta'_j\} = \frac{1}{V_m} [G_{jn}^{rm}] \left\{ \frac{\tau_n^m}{2} \right\} \quad r, m = 0, 1, 2, \dots$$

$$n = m+1, m+3, \dots, j = r+1, r+3, \dots \quad (14)$$

where the ground influence coefficients matrix $[G]$ is defined as

$$[G] = [A] [B] \quad (15)$$

Now, the in-ground-effect inflow coefficients are obtained as

$$\{\alpha'_j\}^{IGE} = \{\alpha'_j\} - \{\beta'_j\} \quad (16)$$

where $\{\alpha\}$ and $\{\beta\}$ are determined for a given rotor load distribution from equations (3) and (14), respectively. If we neglect the unsteady effect of rotor pressure perturbation, a quasi-steady model can be obtained by substituting equations (4) and (14) into equation (15) as

$$\{\alpha'_j\}^{IGE} = \frac{1}{V_m} ([L_{jn}^{rm}] - [G_{jn}^{rm}]) \left\{ \frac{\tau_n^m}{2} \right\} \quad (17)$$

Finally, the distribution of in-ground-effect induced velocity at rotor disk is obtained as

$$w^{IGE} = \sum_r \sum_{j=r+1, r+3, \dots} \bar{P}_j^r(v) [(\alpha_j^{rc})^{IGE} \cos(r\psi) + (\alpha_j^{rs})^{IGE} \sin(r\psi)] \quad (18)$$

3. Pressure Perturbation due to the Ground Motion

In the new finite-state ground effect model, the influence of the ground is represented by a spatially distributed pressure perturbation, Φ_G . In dynamic ground effect, an additional pressure perturbation needs to be used to capture the effect of the motion of the ground plane on the rotor inflow. This suggests a division of the ground pressure into two parts (i.e., the part due to static presence, denoted as Φ_G^S , and the part due to the ground motion, denoted as Φ_G^D). Then the ground pressure perturbation can be expressed as

$$\Phi_G = \Phi_G^S + \Phi_G^D \quad (19)$$

For an incompressible potential flow, the ground pressure perturbation can also be thought of the acceleration potential, and each part satisfies Laplace's equation. This allows us to express both Φ_G^S and Φ_G^D as expansions of associated Legendre functions in ellipsoidal coordinate system at the ground plane.

For the pressure perturbation due to the static presence of the ground plane, a source-like distribution has been assumed as in previous section with $(l+k)$ even in equation (5), i.e.

$$\Phi_G^S = \frac{1}{2} \sum_{l=0}^{\infty} \sum_{k=l, l+2, \dots}^{\infty} \bar{P}_k^l(\hat{v}) \bar{Q}_k^l(i\hat{\eta}) [\sigma_k^{lc} \cos(l\hat{\psi}) + \sigma_k^{ls} \sin(l\hat{\psi})] \quad (20)$$

where the ground pressure coefficients, σ 's, are related to the rotor pressure coefficients, τ 's, as in equation (8) by applying the pressure boundary condition

$$\Phi_G^S = \Phi_R \quad (21)$$

at the ground surface, i.e., at $\hat{\eta} = 0$.

For a moving ground plane, the ground velocity, denoted as g , is defined to be the distribution of the normal component of the local velocity of the ground plane, positive upward and normalized with respect to rotor tip speed, ΩR . The part of such a moving ground plane within the footprint of the rotor wake can be thought of as a turning fan working in the induced flow stream of the helicopter rotor, and having an induced velocity of itself which is equal to g at the ground plane. Based on this analogy, the pressure perturbation due to the ground motion must have a discontinuity across the ground plane, denoted as $\Delta\Phi_G^D$. This implies that the pressure perturbation due to ground motion needs be expanded using associated Legendre functions \bar{P}_i^p and \bar{Q}_i^p with $(p+i)$ odd. The pressure discontinuity due to ground motion is illustrated in Figure 4(a).

The 'ground fan' is assumed to be sharing a common mass flow parameter, V_m , with the helicopter rotor, and the ground velocity g is assumed to be small in magnitude compared to V_m . For a helicopter in hovering or low speed flight, it can also be assumed that the rotor induced flow stream passes the 'ground fan' in a direction approximately perpendicular to the ground plane. Based on the above assumptions, the momentum theory gives the following equation

$$\Delta\Phi_G^D = V_m g \quad (22)$$

for relating the pressure discontinuity of the 'ground fan' with the ground velocity. The above equation suggests that the part of pressure perturbation due to ground motion can be expressed as

$$\Phi_G^D = \frac{1}{2} V_m \sum_{p=0}^{\infty} \sum_{i=p+1, p+3, \dots}^{\infty} \bar{P}_i^p(\hat{v}) \bar{Q}_i^p(i\hat{\eta}) [\gamma_i^{pc} \cos(p\hat{\psi}) + \gamma_i^{ps} \sin(p\hat{\psi})] \quad (23)$$

where the γ 's are called ground velocity coefficients. The pressure discontinuity across the ground plane can then be obtained from the above expression as

$$\Delta\Phi_G^D = V_m \sum_{p=0}^{\infty} \sum_{i=p+1, p+3, \dots}^{\infty} \bar{P}_i^p(\hat{v}) [\gamma_i^{pc} \cos(p\hat{\psi}) + \gamma_i^{ps} \sin(p\hat{\psi})] \quad (24)$$

Substituting equation (24) into equation (22) and applying the orthogonal property of $\bar{P}_i^p(\hat{v})$'s over the interval $\hat{v} \in [0, 1]$, the ground velocity coefficients can be determined as

$$\gamma_i^{0c} = \frac{1}{2\pi} \int_0^{2\pi} \int_0^1 \bar{P}_i^0(\hat{v}) g(\hat{v}, \hat{\psi}) d\hat{v} d\hat{\psi} \quad \text{for } p=0, i=1, 3, \dots (25a)$$

$$\gamma_i^{pc} = \frac{1}{\pi} \int_0^{2\pi} \int_0^1 \bar{P}_i^p(\hat{v}) \cos(p\hat{\psi}) g(\hat{v}, \hat{\psi}) d\hat{v} d\hat{\psi}$$

$$\gamma_i^{ps} = \frac{1}{\pi} \int_0^{2\pi} \int_0^1 \bar{P}_i^p(\hat{v}) \sin(p\hat{\psi}) g(\hat{v}, \hat{\psi}) d\hat{v} d\hat{\psi} \quad \text{for } p>0, i=p+1, p+3, \dots (25b)$$

In general, the velocity distribution of a rigid ground plane with small angular motion can be written as

$$g = g_0 + g_c \hat{r} \cos \hat{\psi} + g_s \hat{r} \sin \hat{\psi} \quad (26)$$

where g_0 is the heaving velocity, and g_c and g_s are the pitching and the rolling angular velocities of the ground plane, respectively. Substituting equation (26) into equation (25), the ground velocity coefficients, γ 's, are obtained for a full ground effect case as

$$\gamma_i^{0c} = g_0 \int_0^1 \bar{P}_i^0(\hat{v}) d\hat{v} \quad i=1, 3, 5, \dots (27a)$$

$$\gamma_i^{1c} = g_c \int_0^1 \sqrt{1-\hat{v}^2} \bar{P}_i^1(\hat{v}) d\hat{v}$$

$$\gamma_i^{1s} = g_s \int_0^1 \sqrt{1-\hat{v}^2} \bar{P}_i^1(\hat{v}) d\hat{v} \quad i=2, 4, 6, \dots (27b)$$

$$\gamma_i^{pc} = \gamma_i^{ps} = 0 \quad \text{for } p > 1 (27c)$$

The spatial distribution of the pressure perturbation due to the ground motion can be determined by substituting equation (27) into equation (23). For example, for a ground velocity of $g^* = g_0^* = 0.09$ where the superscript * represents the normalization with respect to $\sqrt{C_T}/2$, the distributions of the pressure perturbations along the rotor z-axis due to a rotor and a moving ground are shown in Figure 4(b) at the instance when $h = 1.0$. It can be seen from the figure that the pressure perturbations due to the static presence and the motion of the ground plane have different spatial distributions. The static part has a source-like distribution while the dynamic part has a pressure-jump across the ground plane. Moreover, the dynamic part decays faster than the static part above the ground plane.

4. Ground Motion Influence Coefficient Matrix

Equation (19) for ground pressure perturbation due to a moving ground plane suggests that the ground interference velocity at the rotor disk can be written as a superposition of two parts,

$$w_G = w_G^S + w_G^D \quad (28)$$

Neglecting the unsteady part of the ground pressure perturbation, the ground interference velocity at rotor disk can be obtained from the momentum theory for incompressible potential flow as

$$w_G^S = \frac{1}{V_\infty} \int_0^\infty \frac{\partial \Phi_G^S}{\partial z} d\xi \quad (29)$$

and

$$w_G^D = \frac{1}{V_\infty} \int_0^\infty \frac{\partial \Phi_G^D}{\partial z} d\xi \quad (30)$$

where ξ is the coordinate along a stream-line starting from rotor disk, positive upstream.

Analogous to the rotor induced velocity, the above two parts of ground interference velocity can be expressed as

$$w_G^S = \sum_r \sum_{j=r+1, r+3, \dots} \bar{P}_j^r(v) [(\beta_j^{rc})^S \cos(r\psi) + (\beta_j^{rs})^S \sin(r\psi)] \quad (31)$$

and

$$w_G^D = \sum_r \sum_{j=r+1, r+3, \dots} \bar{P}_j^r(v) [(\beta_j^{rc})^D \cos(r\psi) + (\beta_j^{rs})^D \sin(r\psi)] \quad (32)$$

Expression for the ground interference velocity coefficients in equation (29) due to the static presence of the ground plane can be obtained as in equation (8), i.e.,

$$\begin{Bmatrix} \beta_j^{rc} \\ \beta_j^{rs} \end{Bmatrix}^S = \frac{1}{V_m} \begin{bmatrix} [(G_{jn}^{rm})^{cc}] & [(G_{jn}^{rm})^{cs}] \\ [(G_{jn}^{rm})^{sc}] & [(G_{jn}^{rm})^{ss}] \end{bmatrix} \begin{Bmatrix} \tau_n^{mc} / 2 \\ \tau_n^{ms} / 2 \end{Bmatrix} \quad \begin{matrix} r, m = 0, 1, 2, \dots \\ j = r+1, r+3, \dots; n = m+1, m+3, \dots \end{matrix} \quad (33)$$

Substituting equations (23) and (32) into equation (30), and applying the orthogonal property of $\bar{P}_j^r(v)$ at the rotor disk, the ground interference velocity coefficients in equation (32) due to the ground motion can be related to the ground velocity coefficients γ 's in a matrix form as

$$\begin{Bmatrix} \beta_j^{rc} \\ \beta_j^{rs} \end{Bmatrix}^D = \begin{bmatrix} [(C_{ji}^{rp})^{cc}] & [(C_{ji}^{rp})^{cs}] \\ [(C_{ji}^{rp})^{sc}] & [(C_{ji}^{rp})^{ss}] \end{bmatrix} \begin{Bmatrix} \gamma_i^{pc} / 2 \\ \gamma_i^{ps} / 2 \end{Bmatrix} \quad \begin{matrix} r, p = 0, 1, 2, \dots \\ j = r+1, r+3, \dots; i = p+1, p+3, \dots \end{matrix} \quad (34)$$

Equation (34) can also be written as

$$\{\beta_j^r\}^D = [C_{ji}^{rp}] \left\{ \frac{\gamma_i^p}{2} \right\} \quad (34a)$$

where the matrix $[C]$ is the so-called ground motion influence coefficients matrix, which relates the part of the ground interference velocity distribution at the rotor disk to the velocity of the ground plane. Expressions for elements of the $[C]$ matrix can be obtained as,

$$\begin{aligned} (C_{ji}^{0p})^{cc} &= \frac{1}{2\pi} \int_0^{2\pi} \int_0^1 \bar{P}_j^0(v) \int_0^\infty \frac{\partial}{\partial z} [\bar{P}_i^p(\hat{v}) \bar{Q}_i^p(i\hat{\eta}) \cos(p\hat{\psi})] d\xi dv d\psi \\ (C_{ji}^{0p})^{cs} &= \frac{1}{2\pi} \int_0^{2\pi} \int_0^1 \bar{P}_j^0(v) \int_0^\infty \frac{\partial}{\partial z} [\bar{P}_i^p(\hat{v}) \bar{Q}_i^p(i\hat{\eta}) \sin(p\hat{\psi})] d\xi dv d\psi \end{aligned} \quad \text{for } r = 0 \quad (35a)$$

$$\begin{aligned} (C_{ji}^{rp})^{cc} &= \frac{1}{\pi} \int_0^{2\pi} \int_0^1 \bar{P}_j^r(v) \cos(r\psi) \int_0^\infty \frac{\partial}{\partial z} [\bar{P}_i^p(\hat{v}) \bar{Q}_i^p(i\hat{\eta}) \cos(p\hat{\psi})] d\xi dv d\psi \\ (C_{ji}^{rp})^{cs} &= \frac{1}{\pi} \int_0^{2\pi} \int_0^1 \bar{P}_j^r(v) \cos(r\psi) \int_0^\infty \frac{\partial}{\partial z} [\bar{P}_i^p(\hat{v}) \bar{Q}_i^p(i\hat{\eta}) \sin(p\hat{\psi})] d\xi dv d\psi \\ (C_{ji}^{rp})^{sc} &= \frac{1}{\pi} \int_0^{2\pi} \int_0^1 \bar{P}_j^r(v) \sin(r\psi) \int_0^\infty \frac{\partial}{\partial z} [\bar{P}_i^p(\hat{v}) \bar{Q}_i^p(i\hat{\eta}) \cos(p\hat{\psi})] d\xi dv d\psi \\ (C_{ji}^{rp})^{ss} &= \frac{1}{\pi} \int_0^{2\pi} \int_0^1 \bar{P}_j^r(v) \sin(r\psi) \int_0^\infty \frac{\partial}{\partial z} [\bar{P}_i^p(\hat{v}) \bar{Q}_i^p(i\hat{\eta}) \sin(p\hat{\psi})] d\xi dv d\psi \end{aligned} \quad \text{for } r > 0 \quad (35b)$$

where, the transformation between rotor and ground ellipsoidal coordinates

$$(\hat{v}, \hat{\eta}, \hat{\psi}) = F(v, \eta = 0, \psi) \quad (36)$$

is used to obtain the above integrals.

Because of the assumptions made in the previous section for equation (22), the present model for ground motion is valid only for the hovering and very low speed forward flight. In these cases, the skew angle of the rotor wake is approximately equal to zero, and the free-stream is assumed to be along the rotor z-axis. Thus we have

$$\frac{\partial}{\partial z} = -\frac{\partial}{\partial \xi} \quad (37)$$

which simplifies the expressions for the elements of the $[C]$ matrix as

$$\begin{aligned}
(C_{ji}^{0p})^{cc} &= \frac{1}{2\pi} \int_0^{2\pi} \int_0^1 \bar{P}_j^0(v) [\bar{P}_i^p(\hat{v}) \bar{Q}_i^p(i\hat{\eta}) \cos(p\hat{\psi})]_{r=0} dv d\psi \\
(C_{ji}^{0p})^{cs} &= \frac{1}{2\pi} \int_0^{2\pi} \int_0^1 \bar{P}_j^0(v) [\bar{P}_i^p(\hat{v}) \bar{Q}_i^p(i\hat{\eta}) \sin(p\hat{\psi})]_{r=0} dv d\psi \\
(C_{ji}^p)^{cc} &= \frac{1}{\pi} \int_0^{2\pi} \int_0^1 \bar{P}_j^r(v) \cos(r\psi) [\bar{P}_i^p(\hat{v}) \bar{Q}_i^p(i\hat{\eta}) \cos(p\hat{\psi})]_{r=0} dv d\psi \\
(C_{ji}^p)^{cs} &= \frac{1}{\pi} \int_0^{2\pi} \int_0^1 \bar{P}_j^r(v) \cos(r\psi) [\bar{P}_i^p(\hat{v}) \bar{Q}_i^p(i\hat{\eta}) \sin(p\hat{\psi})]_{r=0} dv d\psi \\
(C_{ji}^p)^{sc} &= \frac{1}{\pi} \int_0^{2\pi} \int_0^1 \bar{P}_j^r(v) \sin(r\psi) [\bar{P}_i^p(\hat{v}) \bar{Q}_i^p(i\hat{\eta}) \cos(p\hat{\psi})]_{r=0} dv d\psi \\
(C_{ji}^p)^{ss} &= \frac{1}{\pi} \int_0^{2\pi} \int_0^1 \bar{P}_j^r(v) \sin(r\psi) [\bar{P}_i^p(\hat{v}) \bar{Q}_i^p(i\hat{\eta}) \sin(p\hat{\psi})]_{r=0} dv d\psi
\end{aligned}$$

for $r = 0$ (38a)

for $r > 0$ (38b)

It should be noticed that the indices are $i = p+1, p+3, p+5, \dots$ for $[C]$ matrix.

Tables 1(a), 1(b), and 1(c) present numerical results for the $[C]$ matrices for the normalized hovering heights of $h = 0.5, 1.0, \text{ and } 1.5$, respectively. Those 6×9 $[C]$ matrices are for two harmonics of both the ground interference velocity ($l = 0, 1$) and the ground velocity coefficients ($p = 0, 1$). Each harmonic of the ground interference velocity has two radial modes ($k = l+1, l+3$), and each harmonic of the ground velocity coefficients has three radial modes ($i = p+1, p+3, p+5$). It can be seen from the table that all the sub-matrices for sine-cosine couplings are zero, and all the sub-matrices for couplings between different harmonics are zero too. This implies that the ground velocity of a certain harmonic affects only the same harmonic inflow at the rotor disk, and the pitching (or rolling) motion of the ground plane affects only the longitudinal (or lateral) inflow distribution at the rotor disk. It also can be seen that the first harmonic sine and cosine sub-matrices are the same, i.e.,

$$[C^{11}]^{cc} = [C^{11}]^{ss} \quad (39)$$

which implies that the effect of ground pitching motion on the longitudinal inflow distribution is the same as that of ground rolling motion on the lateral inflow distribution. In each sub-matrix, the elements gradually decrease in magnitude when the order of radial mode becomes higher. Therefore, each sub-matrix can be truncated to a dimension of 2×2 without undue loss of accuracy.

The variations of the elements of the $[C]$ matrix with hovering height are shown in Figures 5(a) and 5(b) for $[C^{00}]^{cc}$ and $[C^{11}]^{cc}$, respectively. It can be seen that the first diagonal element is dominant in each sub-matrix, which is the same as in $[G]$ matrix. Except for element $(C_{11}^{00})^{cc}$, all the other elements decrease very quickly in magnitude as the hovering height is increased, and become negligible for $h > 1.0$. The decay of element $(C_{11}^{00})^{cc}$ is relatively slow compared to other elements, implying that the influence of ground heaving velocity on the fundamental harmonic inflow at rotor disk is the major portion of the dynamic ground effect. In the following two sections, dynamic ground effect on the rotor inflow is analyzed for a heaving ground plane with a uniformly distributed ground velocity, g . The effect of a ground plane with an arbitrary velocity distribution can easily be analyzed following the same approach.

5. Steady Vertical Motion of the Ground Plane

The dynamic ground effect on the inflow at rotor disk can be introduced by substituting equation (28) into equation (10), i.e.,

$$w^{IGE} = w - w_G^S - w_G^D \quad (40)$$

where w is the out-of-ground-effect rotor induced velocity. With w and w^{IGE} expressed as in equations (2) and (18), respectively, the in-ground-effect inflow coefficients are now obtained as

$$\{\alpha\}^{IGE} = \{\alpha\} - \{\beta\}^S - \{\beta\}^D \quad (41)$$

where $\{\beta\}^S$ and $\{\beta\}^D$ are determined using equations (33) and (34), respectively. For a quasi-steady condition, the in-ground-effect inflow coefficients are obtained as

$$\{\alpha\}^{IGE} = \frac{1}{V_m} ([L] - [G]) \left\{ \frac{\tau}{2} \right\} - [C] \left\{ \frac{\gamma}{2} \right\} \quad (42)$$

for the given rotor pressure coefficients, τ 's, and the ground velocity coefficients, γ 's. The inflow distribution at the rotor disk can then be determined by substituting the in-ground-effect inflow coefficients into equation (18).

In this section, the ground plane is assumed to be moving with a constant velocity relative to the helicopter rotor. This is not a very realistic case, but is helpful for the basic understanding of the dynamic ground effect. The inflow

distributions at the rotor disk for varying ground velocities are shown in Figures 6(a) and 6(b) for hovering heights of $h = 0.9$ and 0.4 , respectively. The g^* denotes the velocity of the ground plane normalized with respect to $\sqrt{C_T/2}$, defined as positive upward. It can be seen from the figure that the upward ground velocity strengthens the ground effect by decreasing the inflow velocity over the rotor disk, while the downward motion of the ground plane reduces the ground effect by increasing the rotor inflow. The uniform ground velocity basically introduces an average change of the inflow over the rotor disk, and has very little influence on the radial distribution of the inflow. A comparison between Figures 6(a) and 6(b) shows that the dynamic ground effect due to the ground velocity is remarkably dependent on the rotor height above the ground plane, h . At $h = 0.4$, the ground velocity has a significant influence on the inflow at rotor disk, but such an effect becomes very weak for $h = 0.9$.

The average inflow variations with hovering height are shown in Figure 7 for varying ground velocity, g^* . It can be seen from the figure that the average inflow is decreased from the static ground effect case ($g^* = 0$) by upward ground motion and is increased by downward ground motion. This effect on the average inflow reduces eventually as the hovering height is increased, and becomes negligibly small for $h > 1.5$.

6. Oscillating Heaving Motion of the Ground Plane

In this section, the ground plane is assumed to be heaving periodically like a ship deck at the sea. The rotor height above the ground plane can be described as

$$h = h_0 + \Delta h \sin(\omega t) \quad (43)$$

where h_0 is the mean height and the Δh is the magnitude of oscillation, both normalized with respect to rotor radius, R . The velocity of the ground plane is then

$$g = -\dot{h} = \Delta h \omega \cos(\omega t) \quad (44)$$

For a helicopter rotor hovering above such a heaving ground plane, the induced torque for a steady hover are computed and shown in Figures 8(a), 8(b) and 8(c) for different combinations of h_0 and ω . In the computation, the magnitude of the ground heaving motion is set as $\Delta h = 0.2$. The values of induced torque shown in Figure 8 are normalized with respect to out-of-ground-effect hovering induced torque. The solid lines in the figure are for the results obtained by considering the height variation of equation (43) but neglecting the ground velocity of equation (44). Since the results are normalized with respect to the corresponding out-of-ground-effect value, the normalized induced torque variations become independent of the thrust coefficient when the effect of the ground velocity is neglected. Both variations of the height and the ground velocity have been included in the computation for the results represented as dashed and dotted lines. The dashed lines are for a rotor with thrust coefficient $C_T = 0.01$, which is typical for heavy helicopters. The dotted lines are for a rotor with $C_T = 0.002$, which is typical for small unmanned helicopters like the YAMAHA R-50.

For the results shown in Figure 8(a), the condition is set as $h_0 = 0.5$ and $\omega = \Omega/50$, where Ω is the rotor rotational speed. Therefore, the ground plane completes one cycle of heaving motion while the helicopter rotor rotates through 50 revolutions. It can be seen in the figure that, in such a dynamic ground effect case, there is a remarkable fluctuation in the induced torque of the helicopter rotor. It can be seen that the fluctuation in the induced torque is mainly due to the variation of the rotor height above the ground plane. The ground velocity affects the magnitude as well as the phase of the oscillation of the induced torque. Compared to the effects of the height variation, however, the influence due to the ground velocity is not significant. It is important to notice that the ground velocity exerts a stronger influence on the lightly loaded rotor as compared to that on the heavily loaded rotor.

Figure 8(b) shows results obtained for the condition of $h_0 = 0.5$ and $\omega = \Omega/25$. The increase in the frequency of the ground oscillation amplifies the effects of the ground velocity both on the magnitude and on the phase of the induced torque variation. In particular, the change in magnitude of the induced torque fluctuation appears to be important for the lightly loaded rotor.

The results shown in Figure 8(c) are for the condition of $h_0 = 1.0$ and $\omega = \Omega/50$. The magnitude of the induced torque oscillation is significantly reduced by the increase in the hovering height. The effect of the ground velocity is also significantly reduced. The change in magnitude of the induced torque fluctuation becomes negligibly small. But the phase shift due to the ground velocity is still noticeable.

7. Conclusions

The major conclusions from this study are summarized as follows:

- 1) A new finite-state ground effect model has been extended to modeling of lifting rotors operating above a moving ground plane. In this dynamic ground effect model, the ground interference velocity distribution at the rotor disk is related to the ground velocity distribution by a ground motion influence coefficient matrix, $[C]$.
- 2) Results indicate that the ground velocity affects the induced inflow at the rotor disk. Results also indicate that the influence of the ground velocity is not negligible for lightly loaded helicopter rotors at low hovering height. The results and discussion show that the present finite-state model for ground velocity is qualitatively correct and quantitatively reasonable.

- 3) Due to the assumptions made in the development, the present model can be applied only to hovering and low speed flight. Experimental data is needed for the validation of the present model.

Acknowledgement

This study is supported under the NRTC Center of Excellence in Rotorcraft Technology program at the Georgia Institute of Technology and Washington University.

References

- [1] Newman, E. M., "A New Approach to the Calculation of the Effect of the Ground on the Performance of Rotary Wing Aircraft," AD-736925, November 1971.
- [2] Hayden, J. S., "The Effect of the Ground on Helicopter Hovering Power Required," Proceedings of the AHS 32nd Annual Forum, May 1976.
- [3] Cheeseman, I. C. and Bennett, W. E., "The Effect of the Ground Effect on a Helicopter Rotor in Forward Flight," ARC R&M 3021, September 1955.
- [4] He, C. J., "Development and Application of a Generalized Dynamic Wake Theory for Lifting Rotors," Ph.D. Thesis, Georgia Tech., July 1989.
- [5] Xin, H., Prasad, J. V. R., and Peters, D. A., "Dynamic Inflow Modeling for Simulation of Helicopters Operating in Ground Effect," Proceedings of the 1999 AIAA Modeling & Simulation Technologies Conference, Portland, OR, August 1999.
- [6] Xin, H., Prasad, J. V. R., and Peters, D. A., Itoga, N., Iboshi, N., Nagashima T., "Ground Effect Aerodynamics of Lifting Rotors Hovering above Inclined Ground Plane", Proceedings of the AIAA 17th Applied Aerodynamics Conference, Norfolk, VA, June 1999.

0.4500	0.0720	-0.0027	0.0000	0.0000	0.0000	0.0000	0.0000	0.0000	0.0000
-0.0414	0.1036	0.0371	0.0000	0.0000	0.0000	0.0000	0.0000	0.0000	0.0000
0.0000	0.0000	0.0000	0.2380	0.0563	0.0009	0.0000	0.0000	0.0000	0.0000
0.0000	0.0000	0.0000	-0.0160	0.0507	0.0225	0.0000	0.0000	0.0000	0.0000
0.0000	0.0000	0.0000	0.0000	0.0000	0.0000	0.2380	0.0563	0.0009	0.0000
0.0000	0.0000	0.0000	0.0000	0.0000	0.0000	-0.0160	0.0507	0.0225	0.0000
(a) $h = 0.5$									
0.2436	0.0307	0.0014	0.0000	0.0000	0.0000	0.0000	0.0000	0.0000	0.0000
-0.0480	0.0138	0.0049	0.0000	0.0000	0.0000	0.0000	0.0000	0.0000	0.0000
0.0000	0.0000	0.0000	0.0764	0.0141	0.0012	0.0000	0.0000	0.0000	0.0000
0.0000	0.0000	0.0000	-0.0142	0.0030	0.0016	0.0000	0.0000	0.0000	0.0000
0.0000	0.0000	0.0000	0.0000	0.0000	0.0000	0.0764	0.0141	0.0012	0.0000
0.0000	0.0000	0.0000	0.0000	0.0000	0.0000	-0.0142	0.0030	0.0016	0.0000
(b) $h = 1.0$									
0.1467	0.0131	0.0007	0.0000	0.0000	0.0000	0.0000	0.0000	0.0000	0.0000
-0.0382	0.0013	0.0007	0.0000	0.0000	0.0000	0.0000	0.0000	0.0000	0.0000
0.0000	0.0000	0.0000	0.0292	0.0038	0.0003	0.0000	0.0000	0.0000	0.0000
0.0000	0.0000	0.0000	-0.0076	-0.0002	0.0001	0.0000	0.0000	0.0000	0.0000
0.0000	0.0000	0.0000	0.0000	0.0000	0.0000	0.0292	0.0038	0.0003	0.0000
0.0000	0.0000	0.0000	0.0000	0.0000	0.0000	-0.0076	-0.0002	0.0001	0.0000
(c) $h = 1.5$									

Table.1 [C] Matrices for Hovering in Dynamic Ground Effect for Different Rotor Heights

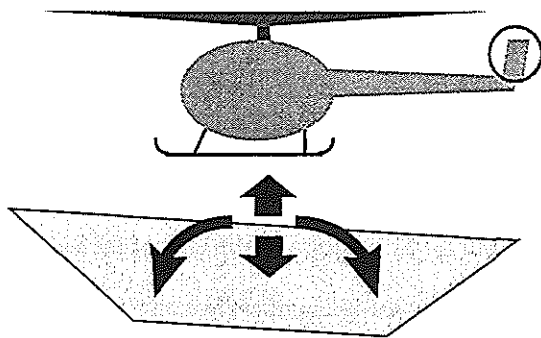


Fig. 1 Dynamic ground effect case

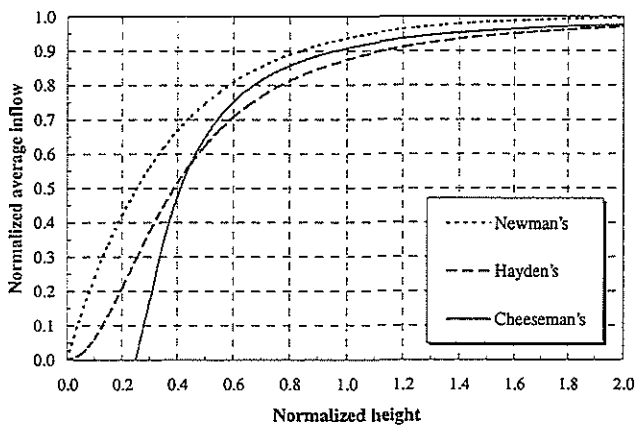


Fig. 2 Empirical^{[1][2]} and analytical^[3] predictions of variation of average inflow with rotor height above the ground

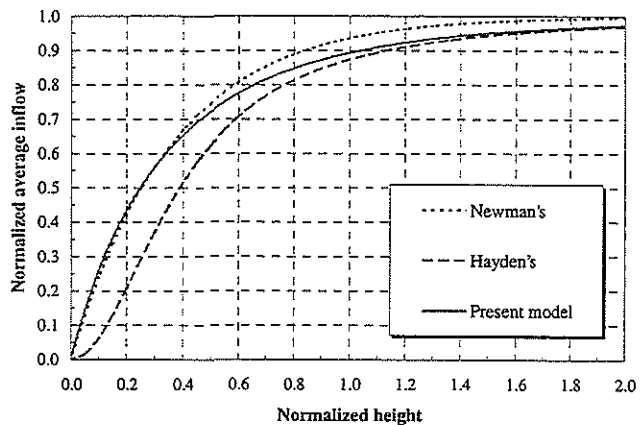
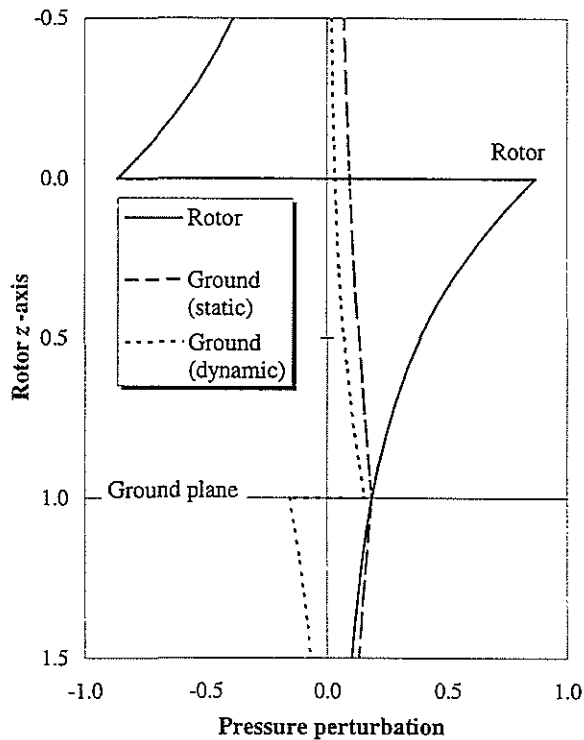
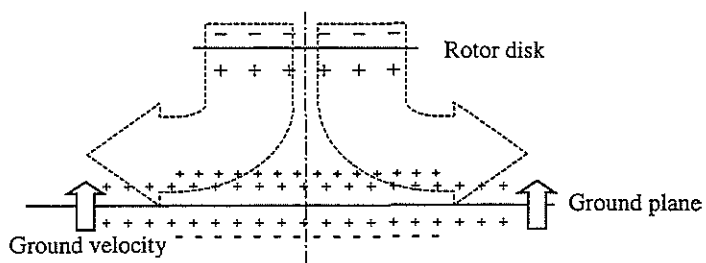


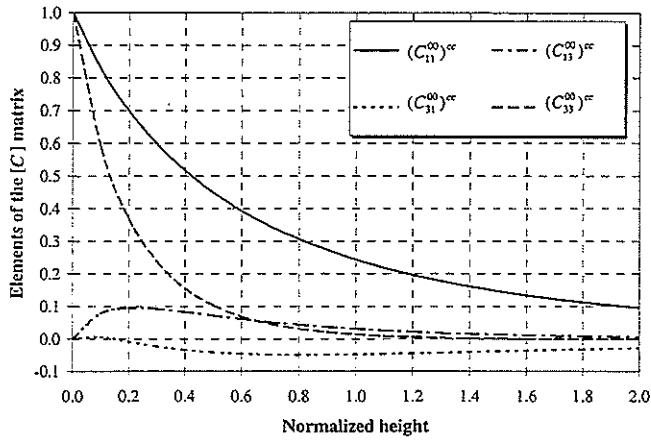
Fig. 3 Aviation of average inflow predicted using a new finite-state ground effect model^[5]



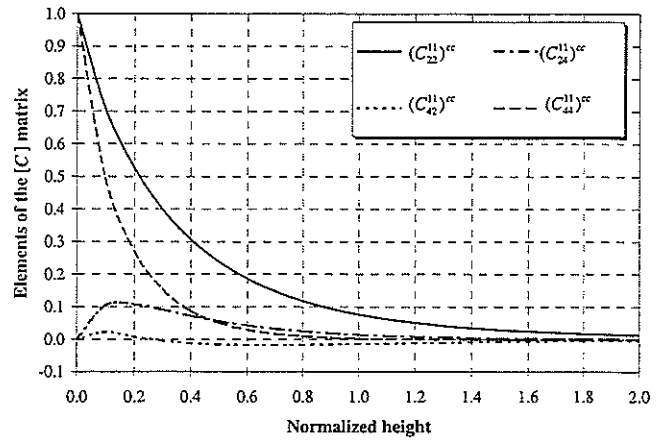
(a) The ground pressure perturbation consists of a mass-source and a pressure-jump

(b) The axial distributions of the pressure perturbations for $h = 1.0$

Fig. 4 The pressure perturbations due to a rotor and a ground plane with upward velocity

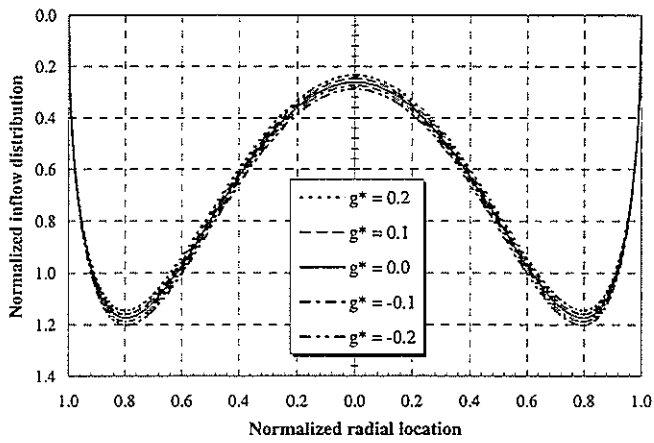


(a) Elements of the sub-matrix $[C^{00}]^{cc}$

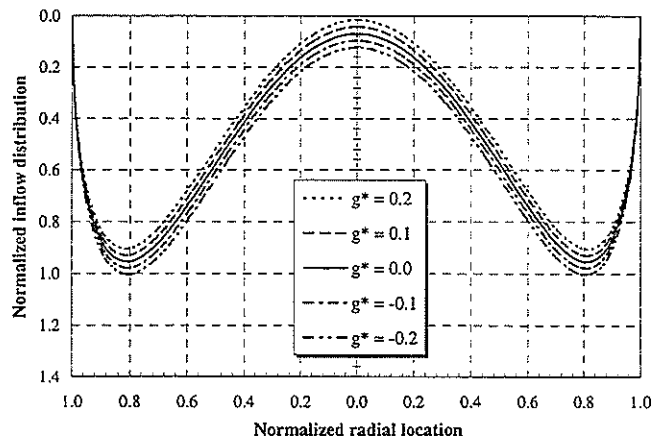


(b) Elements of the sub-matrix $[C^{11}]^{cc}$

Fig. 5 Variation of the $[C]$ matrix with hovering height



(a) $h = 0.9$



(b) $h = 0.4$

Fig. 6 Rotor inflow distributions for different ground velocities, g^*

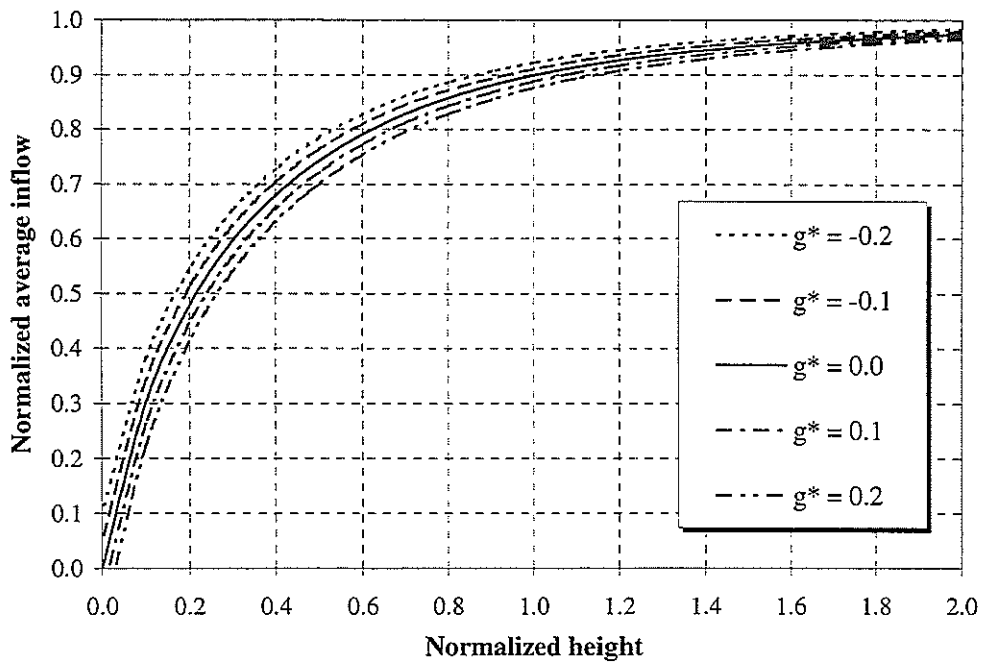
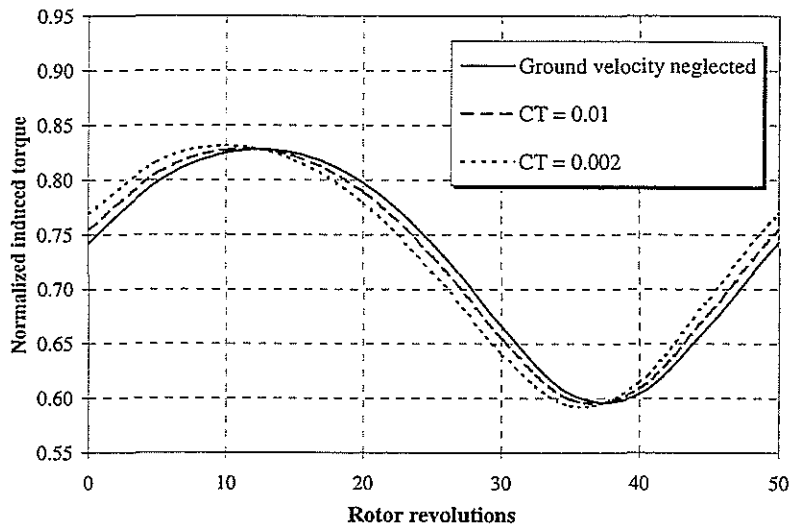
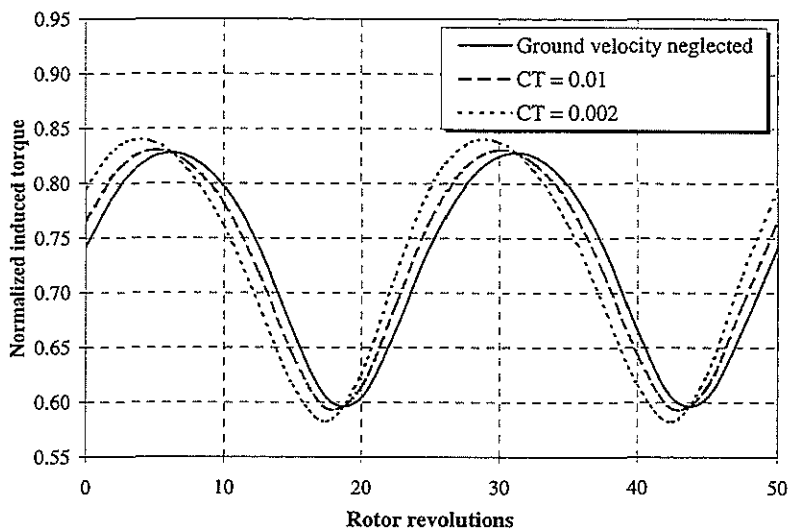


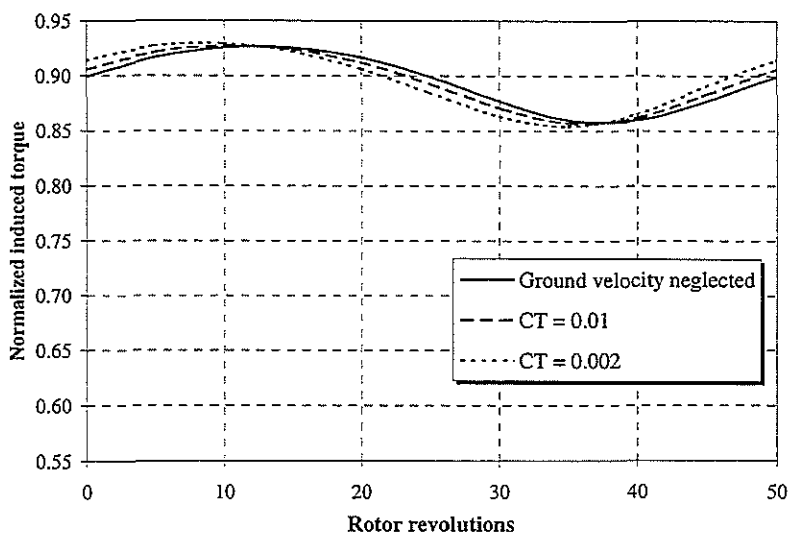
Fig. 7 Rotor average inflow variations for different ground velocities



(a) $h_0 = 0.5, \Delta h = 0.2, \omega = \Omega / 50$



(b) $h_0 = 0.5, \Delta h = 0.2, \omega = \Omega / 25$



(c) $h_0 = 1.0, \Delta h = 0.2, \omega = \Omega / 50$

Fig.8 Induced torque variations due to a heaving ground plane